THE JOURNAL OF PHYSICAL CHEMISTRY Letters

pubs.acs.org/JPCL

Letter

Colloidal Stability of Aqueous Ferrofluids at 10 T

Alex M. van Silfhout, Hans Engelkamp, and Ben H. Erné*

Cite This: J. Phys. Chem. Lett. 2020, 11, 5908–5912

Read Online

ACCESS | Metrics & More | Article Recommendations

ABSTRACT: Magnetic density separation is an emerging recycling technology by which several different waste materials—from plastic products, electronics, or other—can be sorted in a single continuous processing step. Larger-scale installations will require ferrofluids that remain stable at several teslas, high magnetic fields at which colloidal stability was not investigated before. Here we optically monitor the concentration profile of iron oxide nanoparticles in aqueous ferrofluids at a field of 10 T and a gradient of 100 T/m. The sedimentation velocities and equilibrium concentration profiles inform on maintenance or breakdown of colloidal stability, which depends on the concentration and magnetic coupling energy of the nanoparticles. Comparison with results obtained with a small neodymium magnet indicate that stability at moderate fields is predictive of stability at much higher fields, which facilitates the development of new ferrofluids dedicated to magnetic density separation.

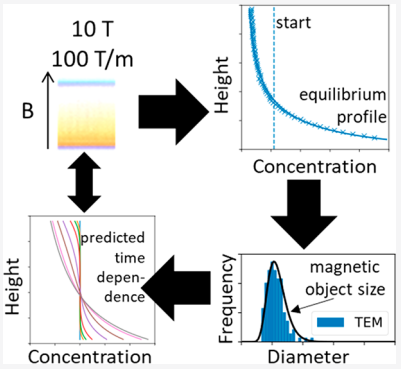

Unsustainable demands on the world's energy and material resources raise the call for practical solutions, and the nanosciences have their part to play. For instance, colloidal dispersions of superparamagnetic nanoparticles enable the separation of solids according to density, which is of great interest in the recycling of mixed waste. How it works is that the ferrofluid is attracted toward a magnet, and consequently, nonmagnetic objects dispersed inside the fluid are effectively repelled by the magnet.[1−3] This approach has long been applied in the diamond industry[4] and in the recovery of nonmagnetic metals,[5] although in both cases separation yields only two fractions, one that sinks and one that floats. In a recent improvement of this approach, different materials float at separate heights inside the fluid and exit in several density fractions in a continuous single-step process (see Figure 1a).[6]

Implementation of magnetic density separation on an industrial scale is complicated by the large distance across which the effective density gradient must be realized. This implies that very strong magnets have to be developed and that the magnetic fluid must remain stable at very high fields. Concretely, to generate a change of $MdB/dz = 1$ g/cm^3 in effective density, a fluid with a magnetization of $M = 1$ kA/m must be submitted to a field gradient of $dB/dz = 10$ T/m;[7] however, to realize this at a distance of 20 cm from the magnet, the magnet must produce at least 2 T to achieve the gradient, plus a further 1 T to magnetize the fluid. At such high fields, paramagnetic salt solutions are stable,[8,9] but their magnetization at 1 T is limited to about 1 kA/m, requiring viscous, concentrated salt solutions, for instance 5 molal $MnCl_2$.[10] In contrast, merely 0.25 vol % concentration of ultrasmall superparamagnetic iron oxide nanoparticles (USPIOs[11]) is sufficient to achieve a magnetization of 1 kA/m at 1 T. For

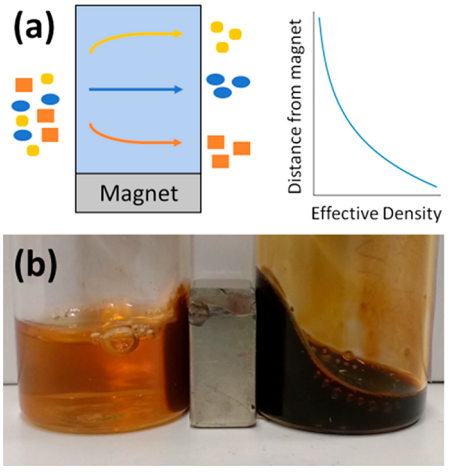

Figure 1. (a) Schematic of magnetic separation of nonmagnetic mixed materials into several density fractions in a single continuous processing step. A magnet magnetizes a magnetic fluid and produces a field gradient, resulting in an effective density gradient.[6] (b) Photograph of two vials of an aqueous magnetic nanofluid with 0.5 vol % citrate-stabilized maghemite particles dispersed in water, with a neodymium magnet between the two. The stable dispersion on the right responds as a whole to the magnet, much more rapidly than the magnetophoresis of individual particles. On the left, however, after addition of 2 M NaCl, the magnetic nanoparticles rapidly separate from the remaining solution.

Received: June 10, 2020
Accepted: July 5, 2020
Published: July 5, 2020

https://dx.doi.org/10.1021/acs.jpclett.0c01804
J. Phys. Chem. Lett. 2020, 11, 5908–5912

ferrofluid behavior, good colloidal stability is crucial, since the alternative is that the magnetic material is rapidly drawn toward the magnet (see Figure 1b). Here we investigate the colloidal stability of dilute aqueous ferrofluids under the extreme field conditions considered for multifraction magnetic density separation on an industrial scale.

Experiments were carried out on three types of aqueous ferrofluid, each with 0.25 vol % iron oxide: a homemade system and two commercial fluids available at larger quantities (see Figure 2a–d). The homemade fluid consisted of a charge-

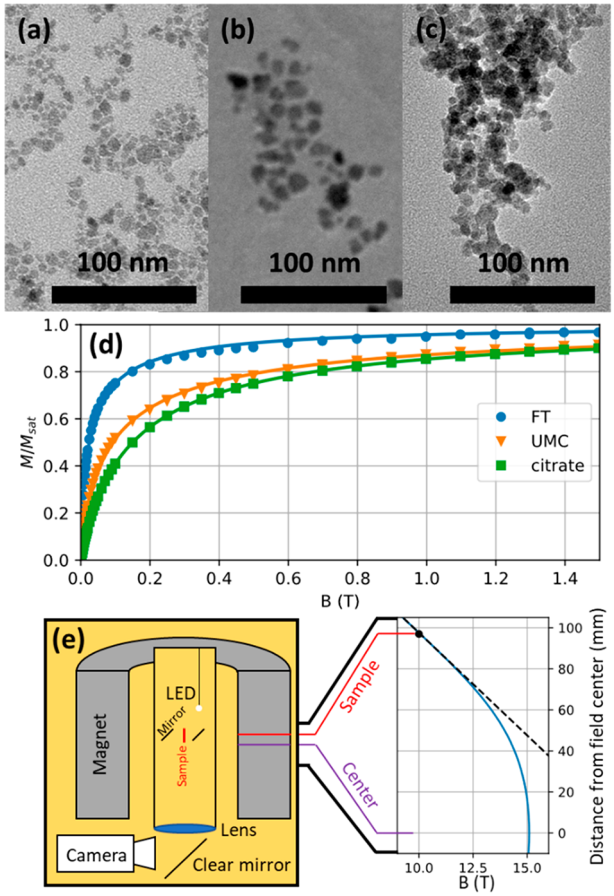

Figure 2. Experimental approach. (a–c) The three studied types of aqueous ferrofluid contained iron oxide nanoparticles mostly in the 5–15 nm diameter range, as observed by electron microscopy: (a) citrate-coated maghemite and (b, c) magnetite particles in the commercial fluids (b) FT and (c) UMC. (d) Curves of sample magnetization M scaled to the saturation magnetization M_{sat} vs external field. The lack of hysteresis upon reversal of the field scanning direction confirms that the particles are superparamagnetic. (e) Setup to characterize colloidal stability at high fields. Concentration gradients in the ferrofluids, contained inside flat glass capillaries, are imaged inside the central bore of a 30 T Bitter magnet. The field strength scales with the electrical current flowing through the magnet, and the relative field gradient depends on the vertical distance from the center of the magnet.

stabilized dispersion of citrate-coated maghemite nanoparticles (γ-Fe_2O_3); when properly prepared, citrate-stabilized ferrofluids have excellent stability,[12] as illustrated by an osmotic pressure that corresponds to separate nanoparticles[13] and by a lack of magnetically induced aggregation, at least below 1 T;[14] size-dependent destabilization occurs upon addition of salt.[15] The commercial ferrofluids were of undisclosed composition, one that we call FT, produced by FerroTec (Santa Clara, CA, U.S.A.), and one that we call UMC, produced by Urban Mining Corporation (Rotterdam, The Netherlands). From our own analyses (magnetometry, pycnometry, infrared spectroscopy), the commercial fluids contain sterically stabilized superparamagnetic iron oxide particles of mainly magnetite (Fe_3O_4) that are slightly larger in size than our homemade maghemite particles.

The colloidal stabilities of the three ferrofluids were tested at fields of up to 10 T and gradients of up to 100 T/m in the setup illustrated in Figure 2e. Samples were lowered into the central bore of a 30 T Bitter magnet, and the field strength and gradient were chosen separately by varying the current through the magnet and changing the vertical sample position. The ferrofluids were inside horizontal flat glass capillaries that were centimeters long with an internal cross section of 50 μm × 1 mm and turned with their thin edge down so that sedimentation occurred across a height of 1 mm. Height-dependent profiles of the transmission of white LED light through 50 μm of ferrofluid were imaged using a CCD camera.

The Bitter magnet could not be switched on instantly. The electrical current through the magnet was ramped up at 80 A/s, corresponding to 44 mT/s at the samples (Figure 3a). The two commercial ferrofluids darkened slightly as soon as the field was turned on, an effect ascribed to light scattering by field-induced dipolar structures,[16−18] which was not seen in the homemade fluid. All three fluids subsequently exhibited sedimentation, with transmission increasing on top and decreasing at the bottom (see Figure 3b–g). Moreover, the optical attenuation-weighted average height of magnetic particles was tracked, indicating initial sedimentation rates of 42 and >3000 nm/s for the citrate-stabilized and commercial fluids, respectively (Figure 3i). Within the first minute, the optical attenuation dropped rapidly in the commercial fluids but not in the homemade fluid. The rapid initial sedimentation in the two commercial fluids is ascribed to the formation of large field-induced dipolar structures.[19−21] Subsequently, sedimentation in the commercial fluids continued at a lower rate (Figure 3i).

To determine the size of the colloidal objects that were still well-dispersed after prolonged sedimentation, the final concentration profiles after 2–3 h were analyzed. Under the assumption that a steady state between magnetic sedimentation and diffusion in the opposite direction was reached at each height, magnetic size distributions were calculated via the method of Berret et al.[14] A log-normal size distribution of superparamagnetic particles was assumed, colloidal interactions were neglected, and the experimentally measured spatial dependence of the magnetic field strength of our magnets was taken into account. Since we were unsure whether sedimentation equilibrium was reached during the relatively short high-field experiments, we also measured profiles after 200 h of equilibration on neodymium magnets and compared the low- and high-field results.

Size distributions obtained from equilibrium profiles on the neodymium magnets are shown in Figure 4. Size distributions measured by transmission electron microscopy (TEM) and magnetometry (VSM) are presented for comparison. The latter were obtained by fitting magnetization curves to log-normal distributions[22] of the magnetic dipole moment, $m = m_b \pi D^3/6$, where D is the diameter and m_b is equal to 430 kA/m for maghemite[23] and 480 kA/m for magnetite.[24] In the case of the homemade citrate-stabilized fluid, the three independ-

https://dx.doi.org/10.1021/acs.jpclett.0c01804
J. Phys. Chem. Lett. 2020, 11, 5908−5912

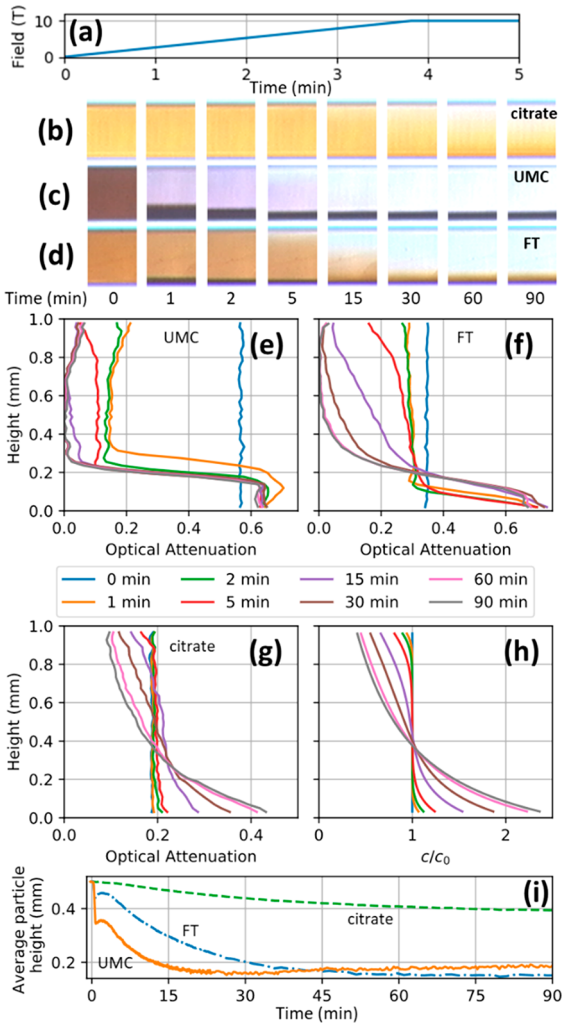

Figure 3. (a) Time dependence of the applied field at the sample location while the Bitter magnet was being turned on. The field gradient scales linearly with the applied field at the sample location and attains 100 T/m within 4 min. (b–d) Simultaneously recorded images of (b) the citrate-stabilized ferrofluid and (c, d) the more rapidly sedimenting (c) UMC and (d) FT ferrofluids. (e–g) Experimental profiles of the optical attenuation in (e) the UMC, (f) the FT, and (g) the citrate-stabilized fluids at 10 T and 100 T/m at the indicated numbers of minutes (corresponding to the images in b–d). (h) Model-based numerical calculations of time-dependent concentration profiles in the citrate-stabilized fluid, expressed in concentration relative to the initial concentration (see panel g). (i) Time dependence of the optical attenuation-weighted average particle height in the citrate-stabilized, FT, and UMC ferrofluids at 10 T and 100 T/m.

ently determined size distributions agree relatively well with each other. In other words, the size of the objects that perform field-driven and Brownian translational motion—as determined from the sedimentation equilibria—corresponds to the physical size observed from electron microscopy and the size of the single magnetic domain. Clearly, these particles are dispersed individually, without aggregation. Moreover, the size distributions calculated from sedimentation equilibrium on neodymium magnets largely explain the time-dependent concentration profiles observed at 10 T, as shown by comparison of the experimental results in Figure 3g with the numerical simulation results in Figure 3h. A caveat is that the particles sedimented a bit more slowly than expected from the

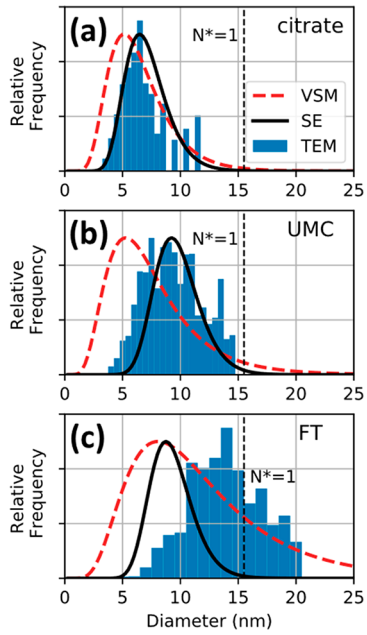

Figure 4. Volume-weighted size distributions calculated from magnetometry (VSM), sedimentation equilibrium profiles (SE), and electron microscopy (TEM) for (a) the citrate-stabilized fluid, (b) the UMC fluid, and (c) the FT fluid. VSM gives the single magnetic domain size, independent of whether the particles are separate or aggregated. SE gives the size of the independently moving objects, single particles or aggregates. The TEM particle size is slightly larger than the VSM size because of a nonmagnetic oxide layer. The vertical dotted lines correspond to the $N^* = 1$ stability criterion.

particle dipole moment and Stokes drag of a sphere. We ascribe the larger hydrodynamic size to a thin layer of nonmagnetic iron oxide, known to be present in such particles,[25] and to the nonspherical shape of the particles.[26]

The sedimentation equilibrium sizes of particles in the top part of the FT fluid significantly differ from those expected from TEM and magnetometry (Figure 4c). These sedimentation equilibrium sizes, however, correspond more closely to the low sedimentation rate after the rapid initial sedimentation (Figure 3i). Apparently, the sediment now contains the largest particles, and the smaller particles remain dispersed above the sediment.

Since the high-field results in Figure 3g,i could be rationalized in terms of the sedimentation size distributions obtained at low fields (Figure 4, SE), the same general requirements for colloidal stability appear to apply at low and high fields. This can be explained in terms of theory of dipolar chaining. The two parameters that determine the presence of dipolar chains in dispersions of dipolar hard spheres are the magnetic coupling energy and the concentration.[27,28] The magnetic coupling energy U_{dip} is the magnetic interaction upon contact between two dipolar spheres in a head-to-tail configuration: $U_{dip} = -\mu_0 m^2/[2\pi(D + 2\delta)^3]$, where $\mu_0 = 4\pi \times 10^{-7}$ J A^{-2} m^{-1} is the permeability of free space, $m = m_b \pi D^3/6$ is the dipole moment in units of A m^2, and D is the physical diameter of the particles, not including a nonmagnetic shell of thickness δ.[20] When the coupling energy is sufficiently small compared with the thermal energy k_BT (where $k_B = 1.38 \times 10^{-23}$ J/K is Boltzmann's constant and T is the absolute temperature), thermal motion of the particles in the solvent suffices to disconnect two magnetically aligned particles, so

https://dx.doi.org/10.1021/acs.jpclett.0c01804
J. Phys. Chem. Lett. 2020, 11, 5908–5912

that dipolar structures neither persist at zero field nor grow in an external field. Concentration, on the other hand, affects the entropic cost of dipolar chaining.

From the thermodynamics of dipolar hard spheres, a criterion for the occurrence of dipolar chains can be formulated: $N^* = [\phi \exp(\Gamma - 1)]^{1/2}$ must be greater than unity, where $\Gamma = -U_{dip}/(k_BT)$ and ϕ is the volume fraction of particles.[29] Our systems are polydisperse, and the particles are not hard spheres, but nevertheless, from their overall volume fraction of $\phi \sim 0.0025$, assuming a bulk magnetization of ~450 kA/m for iron oxide[23,24] and a nonmagnetic shell of 1 nm on each particle, the $N^* = 1$ criterion corresponds to particles having a magnetic core with a diameter of 15.5 nm. Such particles constitute less than 1% of the volume distribution of citrate-stabilized particles prepared via coprecipitation;[25] however, in the FT fluid they represent up to one-third, a fraction on the order of the amount of magnetic material that rapidly sediments while the high-field magnet is being turned on (Figure 3). The criterion for the occurrence of dipolar chains of monodisperse dipolar spheres thus also seems to be useful as an approximate stability criterion for polydisperse real ferrofluids at fields of several teslas. In practice, rather than chemically synthesizing nanoparticles that fulfill this condition from the start, an alternative approach would be to improve a ferrofluid of lesser stability by treating it at high magnetic fields, thus rapidly drawing the particles that do not fulfill the stability condition toward the magnet.[30]

In conclusion, optimal stability is indeed achievable with dilute aqueous magnetic nanofluids at fields of up to 10 T and gradients of up to 100 T/m. Our aqueous citrate-stabilized maghemite ferrofluid consists of separately dispersed particles, both on a neodymium magnet (0.3−0.5 T, gradient of ~20 T/m) and at much higher fields produced by a Bitter magnet (up to 10 T, gradients of up to 100 T/m). In a ferrofluid of lesser stability, the largest iron oxide nanoparticles and their chemical aggregates rapidly separate from solution, and smaller particles remain well-dispersed because their concentrations and dipolar coupling energies are too low for field-induced dipolar structure formation. These insights are useful for the development of new ferrofluids suitable for magnetic density separation. Implementation on an industrial scale, however, also depends on many other considerations, not least of which are the economic aspects of building a high-field setup and feeding it with large quantities of high-quality ferrofluid.

EXPERIMENTAL METHODS

All of the experiments were performed at 25 °C, with the ionic strength of the aqueous ferrofluids set to 10 mM. We detailed our synthesis of citrate-stabilized maghemite dispersions elsewhere,[31] largely following well-known recipes by Massart[32] and Dubois et al.[33] Our approach to study sedimentation on neodymium magnets using a LUMiReader X-ray analyzer (LUM, Berlin, Germany) operating at 17.48 keV was described in ref 31. Transmission electron microscopy was performed on a Tecnai 20 microscope at 200 kV, and magnetization curves were measured with a Microsense EZ-9 vibrating sample magnetometer. The high-field stability experiments were performed at the High Field Magnet Laboratory Nijmegen (cell 1[34]).

The profiles in Figure 3h were simulated by dividing the sample into bins of thickness $\Delta h = 3$ μm at height h, with each bin having its own field strength B and gradient dB/dh (from field measurements on our magnets) and its own different concentrations of particles of different sizes. Three size-dependent forces[35] were taken into account to keep track of the transfer of differently sized particles from one bin to the other: magnetic force ($mLdB/dh$, where m is the nanoparticle dipole moment and L is the Langevin factor), frictional force ($6\pi\eta av$, where η is the viscosity of the solvent, a is the hydrodynamic particle radius, and v is the magnetophoretic velocity), and diffusion force ($((k_BT/c)dc/dh$, where dc/dh is the concentration gradient).

AUTHOR INFORMATION

Corresponding Author

Ben H. Erné − *Van 't Hoff Laboratory for Physical and Colloid Chemistry, Debye Institute for Nanomaterials Science, Utrecht University, 3584 CH Utrecht, The Netherlands;* orcid.org/0000-0001-7392-6443; Email: b.h.erne@uu.nl

Authors

Alex M. van Silfhout − *Van 't Hoff Laboratory for Physical and Colloid Chemistry, Debye Institute for Nanomaterials Science, Utrecht University, 3584 CH Utrecht, The Netherlands*

Hans Engelkamp − *High Field Magnet Laboratory (HFML−EMFL), Radboud University Nijmegen, 6525 ED Nijmegen, The Netherlands;* orcid.org/0000-0001-9920-0536

Complete contact information is available at: https://pubs.acs.org/10.1021/acs.jpclett.0c01804

Notes

The authors declare no competing financial interest.

ACKNOWLEDGMENTS

This work is part of the research programme P14-07 with project number 3.1, (partly) financed by the Dutch Research Council (NWO). The authors acknowledge the support of the HFML-RU/NWO-I, member of the European Magnetic Field Laboratory (EMFL). The authors also thank Prof. Rem from TU Delft for recommending that we perform the high-field experiments, Hans Meeldijk for the electron microscopy, and Urban Mining Corporation for support and ferrofluid samples.

REFERENCES

(1) Rosensweig, R. E. Magnetic Fluids. *Annu. Rev. Fluid Mech.* **1987**, *19*, 437−463.

(2) Anton, I.; De Sabata, I.; Vékás, L. Application Oriented Researches on Magnetic Fluids. *J. Magn. Magn. Mater.* **1990**, *85*, 219−226.

(3) Raj, K.; Hirota, Y.; Black, T. Current and Emerging Applications of Ferrofluids. *Magnetohydrodynamics* **2013**, *49*, 568−581.

(4) Vatta, L. Floating Diamonds with Nanomagnetic Particles. *Macromol. Symp.* **2005**, *225*, 221−228.

(5) Khalafalla, S. E.; Reimers, G. W. Separating Nonferrous Metals in Incinerator Residue Using Magnetic Fluids. *Sep. Sci.* **1973**, *8*, 161−178.

(6) Serranti, S.; Luciani, V.; Bonifazi, G.; Hu, B.; Rem, P. C. An Innovative Recycling Process to Obtain Pure Polyethylene and Polypropylene from Household Waste. *Waste Manage.* **2015**, *35*, 12−20.

(7) Murariu, V.; Svoboda, J.; Sergeant, P. The Modelling of the Separation Process in a Ferrohydrostatic Separator. *Miner. Eng.* **2005**, *18*, 449−457.

(8) Mirica, K. A.; Shevkoplyas, S. S.; Phillips, S. T.; Gupta, M.; Whitesides, G. M. Measuring Densities of Solids and Liquids Using Magnetic Levitation: Fundamentals. *J. Am. Chem. Soc.* **2009**, *131*, 10049−10058.

(9) Zhao, P.; Xie, J.; Gu, F.; Sharmin, N.; Hall, P.; Fu, J. Separation of Mixed Waste Plastics via Magnetic Levitation. *Waste Manage.* **2018**, *76*, 46−54.
(10) Phang, S. The Density, Viscosity and Transference Number of Aqueous Manganese Chloride at 298.15 K. *Aust. J. Chem.* **1980**, *33*, 413−7.
(11) Laurent, S.; Forge, D.; Port, M.; Roch, A.; Robic, C.; Vander Elst, L.; Muller, R. N. Magnetic Iron Oxide Nanoparticles: Synthesis, Stabilization, Vectorization, Physicochemical Characterizations, and Biological Applications. *Chem. Rev.* **2008**, *108*, 2064−2110.
(12) Chanteau, B.; Fresnais, J.; Berret, J.-F. Electrosteric Enhanced Stability of Functional Sub-10 nm Cerium and Iron Oxide Particles in Cell Culture Medium. *Langmuir* **2009**, *25*, 9064−9070.
(13) Cousin, F.; Dubois, E.; Cabuil, V. Tuning the Interactions of a Magnetic Colloidal Suspension. *Phys. Rev. E: Stat. Phys., Plasmas, Fluids, Relat. Interdiscip. Top.* **2003**, *68*, 021405.
(14) Berret, J.-F.; Sandre, O.; Mauger, A. Size Distribution of Superparamagnetic Particles Determined by Magnetic Sedimentation. *Langmuir* **2007**, *23*, 2993−2999.
(15) Lefebure, S.; Dubois, E.; Cabuil, V.; Neveu, S.; Massart, R. Monodisperse Magnetic Nanoparticles: Preparation and Dispersion in Water and Oils. *J. Mater. Res.* **1998**, *13*, 2975−2981.
(16) Lakic, M.; Andjelkovic, L.; Suljagic, M.; Vulic, P.; Peric, M.; Iskrenovic, P.; Krstic, I.; Kuraica, M. M.; Nikolic, A. S. Optical Evidence of Field-Induced Ferrofluid Aggregation: Comparison of Cobalt Ferrite, Magnetite, and Magnesium Ferrite. *Opt. Mater.* **2019**, *91*, 279−285.
(17) Jin, J.; Song, D.; Geng, J.; Jing, D. Time-Dependent Scattering of Incident Light of Various Wavelengths in Ferrofluids under External Field. *J. Magn. Magn. Mater.* **2018**, *447*, 124−133.
(18) Rablau, C.; Vaishnava, P.; Sudakar, C.; Tackett, R.; Lawes, G.; Naik, R. Magnetic-Field-Induced Optical Anisotropy in Ferrofluids: A Time-Dependent Light-Scattering Investigation. *Phys. Rev. E* **2008**, *78*, 051502.
(19) Lim, J. K.; Yeap, S. P.; Leow, C. H.; Toh, P. Y.; Low, S. C. Magnetophoresis of Iron Oxide Nanoparticles at Low Field Gradient: The Role of Shape Anisotropy. *J. Colloid Interface Sci.* **2014**, *421*, 170−177.
(20) Leong, S. S.; Ahmad, Z.; Lim, J. Magnetophoresis of Superparamagnetic Nanoparticles at Low Field Gradient: Hydrodynamic Effect. *Soft Matter* **2015**, *11*, 6968−6980.
(21) Schaller, V.; Kräling, U.; Rusu, C.; Petersson, K.; Wipenmyr, J.; Krozer, A.; Wahnström, G.; Sanz-Velasco, A.; Enoksson, P.; Johansson, C. Motion of Nanometer Sized Magnetic Particles in a Magnetic Field Gradient. *J. Appl. Phys.* **2008**, *104*, 093918.
(22) Luigjes, B.; Woudenberg, S. M. C.; de Groot, R.; Meeldijk, J. D.; Torres Galvis, H. M.; de Jong, K. P.; Philipse, A. P.; Erné, B. H. Diverging Geometric and Magnetic Size Distributions of Iron Oxide Nanocrystals. *J. Phys. Chem. C* **2011**, *115*, 14598.
(23) Shokrollahi, H. A. Review of the Magnetic Properties, Synthesis Methods and Applications of Maghemite. *J. Magn. Magn. Mater.* **2017**, *426*, 74−81.
(24) Cornell, R. M.; Schwertmann, U. *The Iron Oxides*; Wiley-VCH, 2003.
(25) Vasilescu, C.; Latikka, M.; Knudsen, K. D.; Garamus, V. M.; Socoliuc, V.; Turcu, R.; Tombácz, E.; Susan-Resiga, D.; Ras, R. H. A.; Vékás, L. High Concentration Aqueous Magnetic Fluids: Structure, Colloidal Stability, Magnetic and Flow Properties. *Soft Matter* **2018**, *14*, 6648−6666.
(26) Carmichael, G. R. Estimation of the Drag Coefficient of Regularly Shaped Particles in Slow Flows from Morphological Descriptors. *Ind. Eng. Chem. Process Des. Dev.* **1982**, *21*, 401−403.
(27) Klokkenburg, M.; Dullens, R. P. A.; Kegel, W. K.; Erné, B. H.; Philipse, A. P. Quantitative Real-Space Analysis of Self-Assembled Structures of Magnetic Dipolar Colloids. *Phys. Rev. Lett.* **2006**, *96*, 037203.
(28) Klokkenburg, M.; Erné, B. H.; Meeldijk, J. D.; Wiedenmann, A.; Petukhov, A. V.; Dullens, R. P. A.; Philipse, A. P. In Situ Imaging of Field-Induced Hexagonal Columns in Magnetite Ferrofluids. *Phys. Rev. Lett.* **2006**, *97*, 185702.
(29) Faraudo, J.; Andreu, J. S.; Camacho, J. Understanding Diluted Dispersions of Superparamagnetic Particles under Strong Magnetic Fields: a Review of Concepts, Theory and Simulations. *Soft Matter* **2013**, *9*, 6654−6664.
(30) Cotae, C. Experimental Method for the Purification and Reconditioning of Ferrofluids. *J. Magn. Magn. Mater.* **1987**, *65*, 242−244.
(31) van Silfhout, A. M.; Erné, B. H. Magnetic Detection of Nanoparticle Sedimentation in Magnetized Ferrofluids. *J. Magn. Magn. Mater.* **2019**, *472*, 53−58.
(32) Massart, R. Preparation of Aqueous Magnetic Liquids in Alkaline and Acidic Media. *IEEE Trans. Magn.* **1981**, *17*, 1247−1248.
(33) Dubois, E.; Cabuil, V.; Boué, F.; Perzynski, R. Structural Analogy between Aqueous and Oily Magnetic Fluid. *J. Chem. Phys.* **1999**, *111*, 7147−7160.
(34) For full specifications, see: https://www.ru.nl/hfml/use-our-facility/experimental/magnets/ (accessed 2019-12-19).
(35) Lim, J.; Lanni, C.; Evarts, E. R.; Lanni, F.; Tilton, R. D.; Majetich, S. A. Magnetophoresis of Nanoparticles. *ACS Nano* **2011**, *5*, 217−226.

https://dx.doi.org/10.1021/acs.jpclett.0c01804
J. Phys. Chem. Lett. 2020, 11, 5908−5912